Appendix 1.

INVESTIGATION OF AXISYMMETRIC FILM AIRBAGS

Contents

1. INTRODUCTION

Driver safety airbag is under consideration, having an axisymmetric shape when inflated. This airbag shape is appropriate for analysis, because a two-dimensional problem may be considered instead of a three-dimensional one in this case. This property of the airbag holds if it does not interact with other objects. Using an axisymmetric model, we can analyze the airbag shape, pressure within, stress state and strength of the airbag shell as a stand-alone mechanical system.

Though, the purpose of the airbag is to protect a man that sits beside it against impacts and other mechanical influences in the case of a car accident. An accident causes parts of the man's body to push into the airbag thus increasing its interior pressure and stresses in its shell. The airbag's shape loses its axial symmetry, and the design model becomes three-dimensional and hard to analyze. If we knew exact shapes of the man's body which contacts with the shell during an accident and exact location of the body, this three-dimensional analysis would have sense. Without knowing the shapes, we have to make idealizations somehow, representing the body as a set of orbed objects, and define locations of their contact with the airbag.

One of possible idealizations of the human body's shape is a paraboloid of revolution, and the most probable location of its contact with the airbag is the center of the latter. Base of airbag can be approximately represented as a plane. In this case, the mechanical model of the system to be analyzed becomes more complicated, but the problem remains axisymmetric.

2. A SYSTEM OF DIFFERENTIAL EQUATIONS FOR THE AIRBAG ANALYSIS

2.1. Formulation of the problem

Determine, by a specific internal pressure within the airbag, the shape of the bag, stresses in the shell, the force that pushes the dies off, and the extent of redundancy of the material that causes formation of folds.

The shell of the airbag that is analyzed is made of a soft film of a constant thickness. The film has a zero stiffness, both flexural and compression. Under tension, the film behaves as an isotropic linearly elastic material. Its relative extensions can be large.

The shell of the airbag is made in such manner that it has a shape of a body of revolution without folds or stresses in the material when there are no external influences. There can be many shapes of this type. One of them is considered to be the initial shape.

In its operational state, the airbag is filled with gas under some pressure. When deriving formulae, we assume the excess internal pressure to be known.

The airbag interacts with two dies, a flat and a rounded one. The airbag is assumed to lie upon a stiff horizontal plane, and the rounded die, a paraboloid of revolution, is located above at some distance from the plane (Fig. 1). The axis of symmetry of the airbag is perpendicular to the plane. The axis of symmetry of the die coincides with the axis of symmetry of the airbag. Thus, the whole system is axially symmetrical.

When the airbag is inflated, annular folded regions can appear in it because the material does not resist the compression.

2.2. Mathematical formulation

Let's put the objects of study into a cylindrical system of coordinates r, θ, z so that the axis of rotation of the airbag and the rounded die coincide with the axis z.

As the airbag is a body of revolution, its shape is completely determined by a fragment of a curve that is the meridional cross-section of the airbag's shell (Fig. 1).

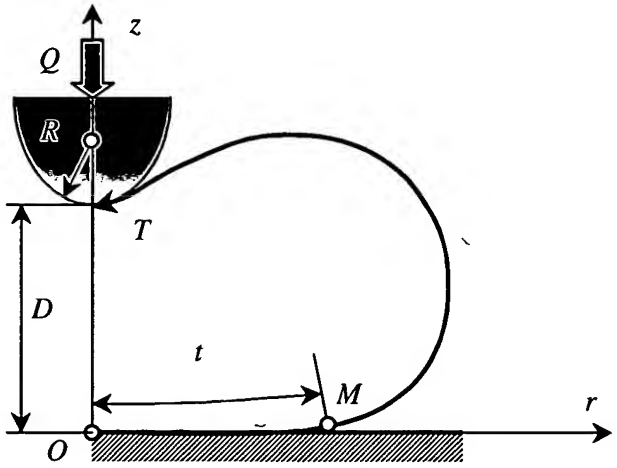

Fig. 1.The meridional cross-section of the airbag

Assume this curve to be defined parametrically using the coordinates $r(t)$, $z(t)$ expressed via the parameter t. The parameter t is the length of the curve fragment from the coordinate origin to the current point M when the airbag is not deformed.

Let the full length of the meridional cross-section curve be T in the initial state, and let the airbag have a shape defined by the coordinates $r_0(t)$, $z_0(t)$ via the parameter t.

Let the foundation plane be located at $z=0$.

Let the rounded die have the shape of a paraboloid of revolution with the meridional cross-section

$$(2.1) \qquad z = \frac{r^2}{2R} + D.$$

The equation shows that the lowest point of the die is at the distance of D from the plane $z=0$, and the radius of curvature of the die in the vicinity of this point is R.

To solve the problem, we will use the method of displacements. According to this choice, formulae will be derived and written. As all variables are functions of the only parameter t, further it is omitted as an argument of the functions.

2.3. Geometric equations

Due to the choice of the arc length as the basic parameter, the following relationship holds:

$$(2.2) \qquad \sqrt{(r_0')^2 + (z_0')^2} = 1;$$

Further below, a stroke denotes the differentiation with respect to t.

The surface of the airbag cannot penetrate to the paraboloid and cannot move down below the plane $z=0$. Therefore, the following conditions must hold:

the inequality limitation imposed by the paraboloid:

$$(2.3) \qquad \frac{r^2}{2R} + D - z \geq 0.$$

the inequality limitation imposed by the stiff plane:

$$(2.4) \qquad z \geq 0$$

The conversion of displacements to elastic relative extensions of the airbag material is expressed by the formulae:

$$(2.5) \qquad \varepsilon_1 = s' - 1 + \eta_1;$$

$$(2.6) \qquad \varepsilon_2 = \frac{r}{r_0} - 1 + \eta_2;$$

where ε_1 is the elastic relative extension of the material in the meridional direction;

ε_2 is the elastic relative extension of the material in the circular direction;

s is the arc length of the meridian of the deformed airbag.

$$(2.7) \qquad s' = \sqrt{(r')^2 + (z')^2}.$$

The dimensionless values η_1 and η_2 need additional explanations. These are fractions of the material's length consumed by the fold formation.

η_1 is the fraction of the length of meridional fibers absorbed by circular folds;

η_2 is the fraction of the length of annular fibers absorbed by meridional folds.

Wavelengths and amplitudes of folds are not the subjects of studies in this report. The folds are assumed to be evenly spread across the surface of the airbag.

Due to folds being formed at a redundant length of fibers, the following inequalities must hold:

$$(2.8) \qquad \eta_1 \geq 0;$$

$$(2.9) \qquad \eta_2 \geq 0.$$

The application of the formulae (2.8) and (2.9) as limitations that express the softness of the material is not commonly known. Usually, one uses conditions of nonnegative stresses. The usage of these formulae is explained by the method of displacements that will be used. The method of displacements must impose limitations upon geometric factors rather than forces or stresses.

2.4. Physical equations

Conventional physical equations are under consideration. We assume that the material of the airbag is linearly elastic, and its stresses can be expressed through elastic extensions by the following formulae:

$$(2.10) \qquad \sigma_1 = \frac{E}{1-\nu^2}(\varepsilon_1 + \nu\varepsilon_2);$$

$$(2.11) \qquad \sigma_2 = \frac{E}{1-\nu^2}(\nu\varepsilon_1 + \varepsilon_2);$$

where E is the elasticity modulus of the film material;

ν is the Poisson ratio of the film material;

σ_1 is the meridional stress;

σ_2 is the annular stress.

2.5. Full energy of the system

We use the variation approach to solution of the problem using the displacement method. This approach seems to be reasonable because the problem contains limitations of the unknown functions in the form of inequalities. These limitations complicate the derivation of governing equations.

The variation approach formalizes this stage of the problem solution, helps choose a consistent system of variables, formulate natural boundary conditions, formulate the conjugate problem if necessary [2], [3], [6] Besides, there is no need to look at the pictures to derive the equilibrium equations.

Let's choose the system of functions that would describe the deformed state of the system completely. These functions can be r, z, η_1, η_2.

Let's use the variation principle of minimum of the full energy of the system. The full energy, including the energy of the load, is expressed by the following functional in this case:

$$(2.12) \qquad \Pi = \int_0^T \left[\frac{\pi r_0 bE}{1-\nu^2}\left(\varepsilon_1^2 + 2\nu\varepsilon_1\varepsilon_2 + \varepsilon_2^2\right) - \pi p r^2 z' \right] dt = \int_0^T f_0(r', z', r, z, \eta_1, \eta_2, t)\, dt .$$

where h is the thickness of the film;

p is the excess pressure in the airbag.

The first term in the brackets represents the elastic energy of the shell's material while the second one the energy of gas as an external load.

The integrand expression should be treated as a function of independent variables r, z, r', z', η_1, η_2, t.

2.6. A principle for deriving the equations

Considering the fact that the problem contains the inequality limitations (2.3), (2.4), (2.8), (2.9) and operates non-smooth (r_0) and discontinuous (r'_0) functions (in the case of an airbag made of two round pieces of film glued together), we will use a pretty general technique known as the principle of maximum of Pontryagin [4], [5]. This technique was developed to solve problems of optimum control, but the Hamiltonian and Lagrangian mechanics can be derived from it as special cases. The principle of maximum of Pontryagin operates deftly with discontinuous controls and limited regions of variable definition.

The problem of optimum control consists of finding n state variables $x_1(t),..,x_n(t)$ and r control variables $u_1(t),..,u_r(t)$ in the specified interval of the argument definition $t_0 \le t \le t_1$ that minimize the given functional:

(2.13) $$x_0 = \int_{t_0}^{t_1} f_0(x_1,..,x_n,u_1,..,u_r,t)\,dt\ ;$$

provided the following equations of state hold:

(2.14) $$x_i' = f_i(x_1,..,x_n,u_1,..,u_r,t) \qquad (i=1,..,n).$$

The stroke denotes the differentiation with respect to t.

The following inequality limitations can be imposed upon the control variables:

(2.15) $$Q_j(u_1,..,u_r) \geq 0 \qquad (j=1,..,k).$$

Let's introduce n conjugate variables $N_1(t),..,N_n(t)$ and build the Hamilton function:

(2.16) $$H(x_1,..,x_n,N_1,..,N_n,u_1,..,u_r,t) = -f_0 + \sum_{i=1}^{n} N_i f_i\ .$$

The principle of maximum of Pontryagin states the following: the optimum control that minimizes the functional (2.13) is achieved at the controls $u_1,..,u_r$ that satisfy the conditions (2.15) and maximize the Hamilton function (2.16) for each t within the interval $t_0 \leq t \leq t_1$.

Also, the following differential dependencies must hold:

(2.17) $$N_i' = -\frac{\partial H}{\partial x_i} \qquad (i=1,..,n);$$

(2.18) $$x_i' = \frac{\partial H}{\partial N_i} \qquad (i=1,..,n).$$

The relationships (2.17), (2.18) are canonical equations of Euler for the problem that is to be solved. The system of equations (2.18) is equivalent to the system of state equations (2.14).

If the inequality limitations are imposed upon the variation of the governing variables:

(2.19) $$S_j(x_1,..,x_n,u_1,..,u_r,t) \geq 0 \qquad (j=1,..,m);$$

then the said approach is true for fragments of the trajectory within a closed region defined by the inequalities (2.19). For fragments of the trajectory located at the boundary of this region, one or more limitations (2.19) become equalities.

In this case, the method of Lagrangian coefficients can be used. Let's denote the set of indexes j that correspond to the limitations (2.19) converted to equalities as J. Let's introduce the Lagrangian coefficients $\mu_j(t)$ ($j \in J$), and use the function below instead of the function f_0:

(2.20) $$F_0 = f_0 - \sum_{j \in J} \mu_j S_j\ .$$

This approach will hold also in the case when the expression below is substituted to the equation (2.20) instead of all or some S_j

(2.21) $$S_j^{(1)} = \sum_{i=1}^{n} \frac{\partial S_j}{\partial x_i} f_i\ ;$$

which represent the limitations of the variable variation in the differential form.

2.7. Formulation of the problem as a problem of optimum control

The problem of minimization of the functional (2.12) at the limitations (2.3), (2.4), (2.8), (2.9) can be treated as a problem of optimum control, if we consider the variables r, z to be the state variables and r', z', η_1, η_2 to be control variables. At the same time, r', z' are assumed to be independent of r, z. Let's denote them as u_r, u_z.

The equations of state will be

(2.22) $r'=u_r$;

(2.23) $z'=u_z$.

The problem includes inequality limitations. Two of them, namely (2.3), (2.4), will be represented in the form (2.21), introducing the notation η_3 and η_4 for the obtained functions:

(2.24) $$\eta_3 = \frac{r}{R}u_r - u_z$$

(2.25) $\eta_4=u_z$.

This form of the limitations is more convenient for the subsequent solution of the problem using the Runge - Kutta method.

We'll introduce Lagrangian coefficients into the set of control variables: μ_1, μ_2, μ_3, μ_4, one per each limitation, and re-write the function (2.20) as follows:

(2.26) $$F_0 = \frac{\pi r_0 bE}{1-\nu^2}\left(\varepsilon_1^2 + 2\nu\varepsilon_1\varepsilon_2 + \varepsilon_2^2\right) - \pi p r^2 u_z - \mu_1\eta_1 - \mu_2\eta_2 - \mu_3\eta_3 - \mu_4\eta_4 .$$

Introducing the conjugate variables N_r, N_z, we will obtain the Hamiltonian function:

(2.27) $$H = -\frac{\pi r_0 bE}{1-\nu^2}\left(\varepsilon_1^2 + 2\nu\varepsilon_1\varepsilon_2 + \varepsilon_2^2\right) + \pi p r^2 u_z + \mu_1\eta_1 + \mu_2\eta_2 + \mu_3\eta_3 + \mu_4\eta_4 + N_r u_r + N_z u_z .$$

The Hamiltonian function is assumed to depend upon the following arguments:

(2.28) $H=H(r, z, N_r, N_z, \eta_1, \eta_2, u_r, u_z, \mu_1, \mu_2, \mu_3, \mu_4, t)$;

where η_3 and η_4 can be expressed via the listed arguments by the formulae (2.24) and (2.25), ε_1 and ε_2 by the formulae (2.5), (2.6).

According to (2.7), we will consider s' to be the function of u_r, u_z:

π, h, E, p are constants.

(2.29) $$s' = \sqrt{u_r^2 + u_z^2}\ ;$$

2.8. Derivation of equations

Using the expression (2.27), we can obtain systems of differential equations for building any fragment of the integral curve, both within the region defined by the inequalities (2.3), (2.4), (2.8), (2.9) and belonging to its boundary. Specifying some of the Lagrangian coefficients to be permanently equal to zero, we will define a boundary manifold to which the integral curve belongs. If some of the Lagrangian coefficients (for example, μ_2) is specified to be zero, its corresponding limitation ($\eta_2 \geq 0$) is not obliged to be an equality. To analyze a fragment of the curve that belongs to the boundary manifold ($\eta_2=0$; $\eta_3=0$), we should leave non-zero only μ_2 and μ_3 in the Hamiltonian function. The rest of the Lagrangian coefficients (μ_1 and μ_4) should be made zero. If all Lagrangian coefficients were made zero, the Hamiltonian function would describe a fragment of the integral curve that lies strictly within the admissible region.

To shorten writing, let's introduce the following notation:

(2.30) $$\rho_0 = \frac{r}{r_0};$$

(2.31) $$\rho_1 = \frac{r}{R};$$

(2.32) $B=2\pi r_0 hE$;

(2.33) $$N_1 = B\frac{\varepsilon_1 + \nu\varepsilon_2}{1-\nu^2};$$

(2.34) $$N_2 = B\frac{\nu\varepsilon_1 + \varepsilon_2}{1-\nu^2}.$$

Let's calculate partial derivatives of the Hamiltonian function needed for the subsequent analysis.

Derivatives with respect to state variables:

(2.35) $$\frac{\partial H}{\partial r} = 2\pi r p u_z + \frac{\mu_3}{R}u_r - \frac{N_2}{r_0};$$

(2.36) $$\frac{\partial H}{\partial z} = 0.$$

Derivatives with respect to conjugate variables:

(2.37) $$\frac{\partial H}{\partial N_r} = u_r;$$

(2.38) $$\frac{\partial H}{\partial N_z} = u_z.$$

Derivatives with respect to control variables:

(2.39) $$\frac{\partial H}{\partial u_r} = N_r + \mu_3\rho_1 - \frac{u_r}{s'}N_1;$$

(2.40) $$\frac{\partial H}{\partial u_z} = N_0 - \mu_3 + \mu_4 - \frac{u_z}{s'}N_1;$$

(2.41) $$\frac{\partial H}{\partial \eta_1} = \mu_1 - N_1;$$

(2.42) $$\frac{\partial H}{\partial \eta_2} = \mu_2 - N_2;$$

Derivatives with respect to Lagrangian coefficients:

(2.43) $$\frac{\partial H}{\partial \mu_1} = \eta_1;$$

(2.44) $$\frac{\partial H}{\partial \mu_2} = \eta_2;$$

(2.45) $$\frac{\partial H}{\partial \mu_3} = \eta_3;$$

(2.46) $$\frac{\partial H}{\partial \mu_4} = \eta_4;$$

Using the formulae (2.17), (2.18) and the expressions (2.35), (2.36), (2.37), (2.38), we can write the system of differential equations for r, z, N_r, N_z.

(2.47) $$r' = u_r;$$

(2.48) $$z' = u_z;$$

(2.49) $$N_r' = -2\pi r p u_z - \frac{\mu_3}{R}u_r + \frac{N_2}{r_0};$$

(2.50) $$N_z' = 0.$$

The further technique of deriving the equations is as follows. Choose the manifold for which we should obtain the differential equations that describe the integral curve. According to considerations of Section 2.7, make some Lagrangian coefficients equal to zero. Compose the system of equations to determine the control variables and non-zero Lagrangian coefficients on the basis of necessary conditions of maximum of the Hamiltonian function, i.e. the conditions of its stationarity. To do that, derivatives with respect to zero Lagrangian coefficients must be excluded from the system of partial derivative (2.39) - (2.46), and the other partial derivatives must be assumed equal to zero.

This system is then resolved with respect to the control variables and non-zero Lagrangian coefficients.

The solutions that have been found are given in Table 1 for six versions of boundary manifolds.

Table 1. Formulae for Lagrangian coefficients and control variables

	No folds		There are folds	
Contact with the upper die	$\mu_1 = -\frac{N_r + \rho_1 N_0}{\sqrt{1+\rho_1^2}}$	$\eta_1=0$	$\mu_1 = -\frac{N_r + \rho_1 N_0}{\sqrt{1+\rho_1^2}}$	$\eta_1= 0$
	$\mu_2=B\Delta$	$\eta_2=0$	$\mu_2= 0$	$\eta_2=-\Delta$
	$\mu_3 = -\frac{N_\Delta}{1+\rho_1^2}$	$u_1 = -\frac{K-\nu\Delta}{\sqrt{1+\rho_1^2}}$	$\mu_3 = -\frac{\rho_1 N_\Delta}{1+\rho_1^2}$	$u_1 = -\frac{K}{\sqrt{1+\rho_1^2}}$
	$\mu_4= 0$	$u_2 = -\frac{\rho_1(K-\nu\Delta)}{\sqrt{1+\rho_1^2}}$	$\mu_4= 0$	$u_2 = -\frac{\rho_1 K}{\sqrt{1+\rho_1^2}}$
Free shell	$\mu_1 = \sqrt{N_r^2 + N_0^2}$	$\eta_1=0$	$\mu_1 = \sqrt{N_r^2 + N_0^2}$	$\eta_1=0$
	$\mu_2=B\Delta$	$\eta_2=0$	$\mu_2=0$	$\eta_2= -\Delta$
	$\mu_3= 0$	$u_1 = \frac{N_r(K-\nu\Delta)}{\sqrt{N_r^2 + N_0^2}}$	$\mu_3= 0$	$u_1 = \frac{N_r K}{\sqrt{N_r^2 + N_0^2}}$
	$\mu_4= 0$	$u_2 = \frac{N_0(K-\nu\Delta)}{\sqrt{N_r^2 + N_0^2}}$	$\mu_4= 0$	$u_2 = \frac{N_0 K}{\sqrt{N_r^2 + N_0^2}}$
Contact with the lower die	$\mu_1=N_r$	$\eta_1=0$	$\mu_1=N_r$	$\eta_1=0$
	$\mu_2=B\Delta$	$\eta_2=0$	$\mu_2=0$	$\eta_2= -\Delta$
	$\mu_3= 0$	$u_1=K-\nu\Delta$	$\mu_3=0$	$u_1=K$
	$\mu_4 = -N_0$	$u_2=0$	$\mu_4= -N_0$	$u_2=0$

This table uses the following notation (also, further below):

(2.51) $N_0=N_z+\pi p r^2$;

(2.52) $N_\Delta=\rho_1 N_r - N_0$;

(2.53) $K = 1+\frac{\mu_1}{B}$;

(2.54) $$\Delta = \rho_0 - 1 + \frac{\nu\mu_1}{B}.$$

To determine K and Δ, the value of μ_1 should be taken from its own boundary manifold.

Table 2. Systems of differential equations for state and conjugate variables

	No folds		There are folds
Contact with the upper die	$r' = -\frac{K - \nu\Delta}{\sqrt{1+\rho_1^2}}$	Transition: $\Delta \geq 0\uparrow$; $\Delta < 0\downarrow$	$r' = -\frac{K}{\sqrt{1+\rho_1^2}}$
	$z' = -\frac{\rho_1 (K - \nu\Delta)}{\sqrt{1+\rho_1^2}}$		$z' = -\frac{\rho_1 K}{\sqrt{1+\rho_1^2}}$
	$N_r' = \frac{B\Delta}{r_0} + \left(2\pi r p \rho_1 - \frac{N_\Delta}{(1+\rho_1^2)R}\right)\frac{K - \nu\Delta}{\sqrt{1+\rho_1^2}}$		$N_r' = \left(2\pi r p \rho_1 - \frac{N_\Delta}{(1+\rho_1^2)R}\right)\frac{K}{\sqrt{1+\rho_1^2}}$
	$N'_z = 0$		$N_\tau' = 0$
	Transition: $N_\Delta \geq 0\uparrow$; $N_\Delta < 0\downarrow$		Transition: $N_\Delta \geq 0\uparrow$; $N_\Delta < 0\downarrow$
Free shell	$r' = \frac{N_r (K - \nu\Delta)}{\sqrt{N_r^2 + N_0^2}}$	Transition: $\Delta \geq 0\uparrow$; $\Delta < 0\downarrow$	$r' = \frac{N_r K}{\sqrt{N_r^2 + N_0^2}}$
	$z' = \frac{N_0 (K - \nu\Delta)}{\sqrt{N_r^2 + N_0^2}}$		$z' = \frac{N_0 K}{\sqrt{N_r^2 + N_0^2}}$
	$N_r' = \frac{B\Delta}{r_0} - \frac{2\pi r p N_0 (K - \nu\Delta)}{\sqrt{N_r^2 + N_0^2}}$		$N_r' = -\frac{2\pi r p N_0 K}{\sqrt{N_r^2 + N_0^2}}$
	$N_\tau' = 0$		$N_\tau' = 0$
	Transition: $N_0 \geq 0\uparrow$; $N_0 < 0\downarrow$		Transition: $N_0 \geq 0\uparrow$; $N_0 < 0\downarrow$
Contact with the lower die	$r' = K - \nu\Delta$	Transition: $\Delta \geq 0\uparrow$; $\Delta < 0\downarrow$	$r' = K$
	$z' = 0$		$z' = 0$
	$N_r' = \frac{B\Delta}{r_0}$		$N_r' = 0$
	$N_\tau' = 0$		$N_\tau' = 0$

Substituting the relationships given in Table 1 to the formulae (2.47) - (2.50), we will obtain the systems of differential equations of interest. They are given in Table 2.

This table lists also conditions of transition from one boundary manifold to another. Three determinant functions are used to do that: N_0, N_Δ and Δ. Alteration of sign of the N_0 function shows the separation of the airbag and the flat die. Alteration of sign of the N_Δ function shows the separation of the airbag and the rounded die. Alteration of sign of the Δ function occurs at the boundary of the smooth and folded regions of the airbag. These functions are the determinant ones for Lagrangian coefficients.

We suggest to use the principle of extension by parameter. If the boundary manifold has been determined correctly in the initial point of integration, then the transition from one boundary manifold to another, according to altered signs of the determinant functions, will have the correct result.

Note that all the relationships have been obtained without any simplifications. Both displacements and relative extensions can be arbitrarily large.

2.9. Boundary conditions

The boundary conditions for the problem to be solved can be formulated in a pretty simple form:

(2.55) $r(0)=0;\ z(0)=0;$

(2.56) $r(T)=0;\ z(T)=D.$

Though, these boundary conditions are inconvenient for use with the methods of Euler or Runge - Kutta. It would be better to know values of all four unknown functions at the same point of the integral curve.

The second inconvenience is that the process of integration can become unstable when the integral curve goes from "soft" folded regions to "stiff" regions without folds, or to regions of contact with the die.

To eliminate this second inconvenience, we suggest the technique of integration "from edges to the middle". According to this technique, two integral curves are searched for using the Euler or Runge - Kutta method. One of them is built for the range of t values $[0..T/2]$. It begins in the initial point and ends in the middle point of the integration interval. The second curve is built for the range of t values $[T..T/2]$. It starts in the initial point and ends, just the same as the second curve, in the middle point of the integration interval. All four unknown functions r, z, N_r, N_z must be consistent in the point $t=T/2$.

To begin the integration, we have to know also values of conjugate variables N_r and N_z, besides knowing the values (2.55), (2.56). Four values of the conjugate variables at the ends must be selected in such manner that the four unknown functions r, z, N_r, N_z be consistent at $t=T/2$. The function N_z is constant on the whole interval of integration, and this facilitates the task to some extent. Its values at the ends of the integration interval are equal: $N_z(0)=N_z(T)$.

There is another difficulty to be mentioned. In the two edge points of the integral curve, at $r=0$, $z=0$ and $r=0$, $z=D$, some auxiliary functions become infinite. Therefore, the integration is better started at some gap from these points. To be definite, let this gap be Δt.

Assuming that the material of the shell is evenly tensioned in the vicinity of the point $r=0$, we can state for this vicinity:

(2.57) $$K=1+\frac{\varepsilon}{1-\nu};$$

(2.58) $$\Delta=\frac{\varepsilon}{1-\nu};$$

(2.59) $$K-\nu\Delta=1+\varepsilon.$$

Then, using the systems of differential equations included in Table 2, we will obtain initial conditions for the point defined by the parameter $t=T-\Delta t$:

(2.60) $$r(T-\Delta t)=\Delta t(1+\varepsilon);$$

(2.61) $$z(T-\Delta t)=D+\frac{(\Delta t)^2}{2R};$$

(2.62) $$N_r(T-\Delta t)=-\Delta t\left(\frac{2\pi hE\varepsilon}{1-\nu}+\frac{N_z}{R}\right);$$

(2.63) $N_z(T-\Delta t) = N_z$.

In the same way, we will obtain the following for the point at $t=\Delta t$:

(2.64) $r(\Delta t) = \Delta t(1+\varepsilon)$;

(2.65) $z(\Delta t) = 0$;

(2.66) $N_r(\Delta t) = \frac{2\pi h E \varepsilon \Delta t}{1-\nu}$;

(2.67) $N_z(\Delta t) = N_z$.

In the point of contact with the upper die, ε is assumed to have its particular value. In the point of contact with the lower die, another value of ε is assumed. Though, values of N_z in those points must be equal.

3. LAWS OF DEFORMATION OF AXISYMMETRIC AIRBAGS

3.1. Assumptions

The design of the system of interest is shown on Fig. 1.

The notation:

R_0 is the radius of the airbag in the non-deformed flat state;

h is the thickness of the film that the shell is made of;

E is the film's elasticity modulus;

ν is the Poisson ratio;

r, θ, z are the coordinates, namely:

r is the radial coordinate;

θ is the angular coordinate;

z is the linear coordinate counted along the rotation axis;

t is the length of the line that connects the coordinate origin and the current point M of the meridional cross-section of the airbag in the non-deformed state;

r_0 is the radial coordinate for the non-deformed airbag;

R is the curve radius of the moving body;

D is the distance between the moving body and the support plane;

Q is the force of pressure of the moving body upon the airbag;

p is the overpressure within the airbag;

V is the volume of the airbag in the deformed state;

σ_1 is the meridional stress;

σ_2 is the circular stress;

η_2 is the fraction of the length of circular fibers absorbed in meridional folds.

As the airbag is made of two flat round sheets of a material of the constant thickness of the radius R_0, the following dependency holds and is used in computations:

(3.1)
$$r_0 = t \quad (t \le R_0)$$
$$r_0 = 2R_0 - t \quad (t > R_0)$$

3.2. The basic design of the airbag

Numerical computations have been done using the units of kilogram-force (kg-f) and centimeter. The following basic airbag design parameters were agreed upon:

(3.2) R_0=35 cm; h=0.01 cm; E=35000 kg-f/cm^2; ν=0.39; R=40 cm; p=0.2 kg-f/cm^2.

Fixed-parameter calculations were done exactly with the basic design. When doing the serial analysis within a certain range of variation of the parameters, the basic design was the central point.

3.3. The dependency between the stress and strain state of the airbag and the material rigidity

A series of calculations was performed for the airbag that did not touch any bodies, with the following source data:

(3.3) R_0=35 cm; h=0.01 cm; ν=0.39; p=0.2 kg-f/cm^2.

The elasticity modulus of the material varied in the range of E=[636..3500000] kg-f/cm^2. The lower boundary of this range is close to the critical value of 593.5 kg-f/cm^2 at which the displacements rise dramatically even at a slight decrease of the elasticity modulus. The upper boundary is 100 times greater than the basic value.

Results of the analysis are represented by charts. The shapes of the airbags depending upon the material's elasticity modulus are shown on Fig. 2 and Fig. 3.

Fig. 2 shows meridional cross-sections of the airbags made of soft films with a low elasticity modulus similar to rubber. At these elasticity modulus values, the airbags inflate immensely, acquiring nearly spherical shapes. Folded regions disappear. The surface of the airbag becomes smooth. Relative extensions of the material are large.

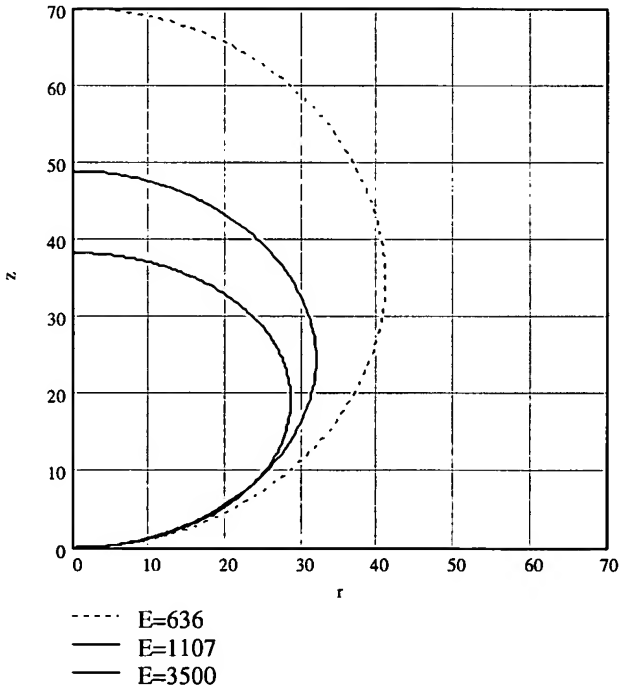

Fig. 2. The airbag shape in the case of a pliable film. R_0=35; h=0.01; ν=0.39; p=0.2

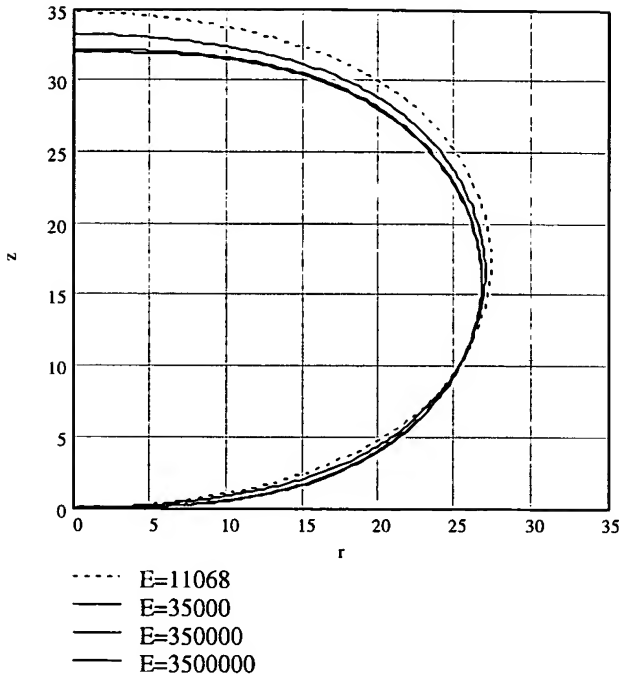

Fig. 3. The airbag shape in the case of a rigid film. R_0=35; h=0.01; ν=0.39; p=0.2

Fig. 3 shows meridional cross-sections of the airbags made of rigid films. The elasticity modulus of the shell film is 10000 kg-f/cm^2 to an almost infinite value. In this series of computations, the airbag shape depends little upon the material's elasticity modulus. The airbag looks like a flattened ellipsoid of revolution with the aspect ratio 0.6:1. There are intensive folds formed in the equatorial region of the airbag.

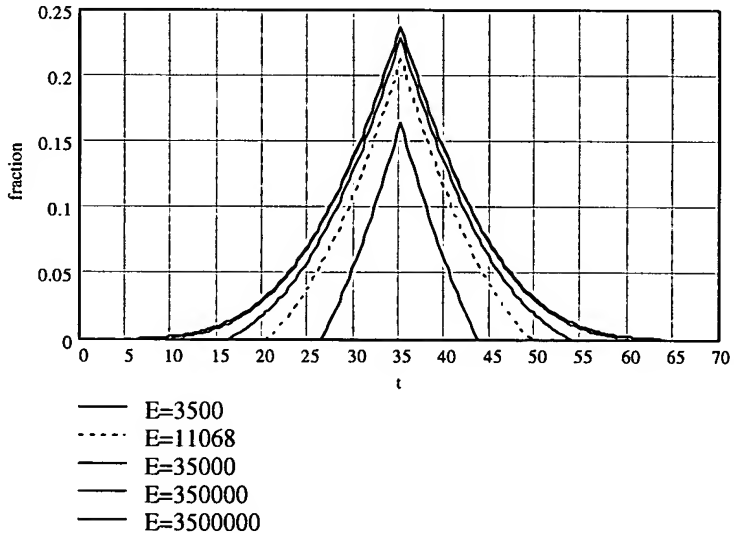

Fig. 4. Regions and intensities of fold formation. R_0=35; h=0.01; ν=0.39; p=0.2

Fig. 4 shows regions where folds are formed and diagrams of the fraction of the circular fiber length of the airbag absorbed by the meridional folds. The argument is the t parameter, the length of the line that goes from the coordinate origin to the current point of the meridional cross-section of the airbag in the non-deformed state (see Fig. 1). The value of the parameter t=0 cm corresponds to the center of the round sheet that lies on the support plane, t=35 cm is the glued seam of the round sheets, t=70 cm is the center of the sheet that faces the man.

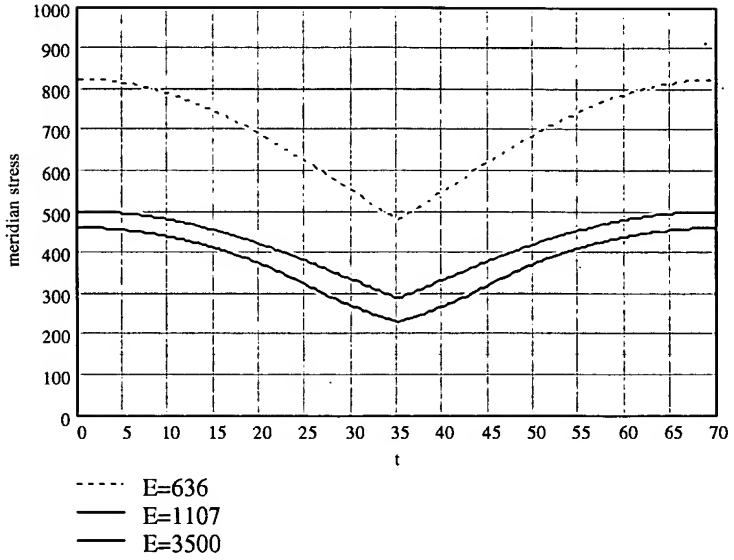

Fig. 5. Meridional stresses for the pliable film. R_0=35; h=0.01; ν=0.39; p=0.2

As you can see from the diagrams, the more rigid the shell material is, the wider area is occupied by the folds, and the more fraction of the circular fiber length is absorbed by the folds. At the elasticity modulus of E=636 kg-f/cm^2 and E=1107 kg-f/cm^2 the folds do not appear at all, and the surface of the airbag becomes smooth.

The stress state of the airbag's shell can be described by meridional and circular stresses. Fig. 5 shows diagrams of meridional stresses in a pliable film, while Fig. 6 shows those in a rigid film.

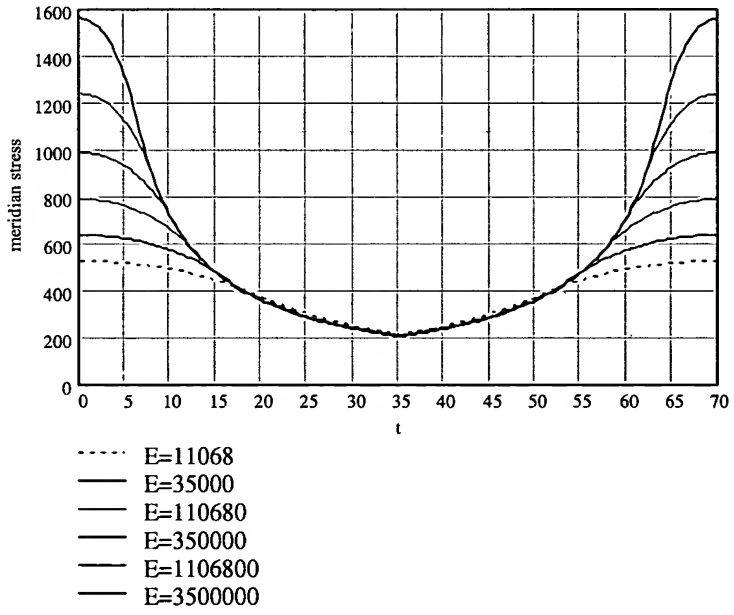

Fig. 6. Meridional stresses in a rigid film. R_0=35; h=0.01; ν=0.39; p=0.2

As the diagrams show, the maximum stresses are found in the central areas of the round sheets. The minimum stresses appear in the seams.

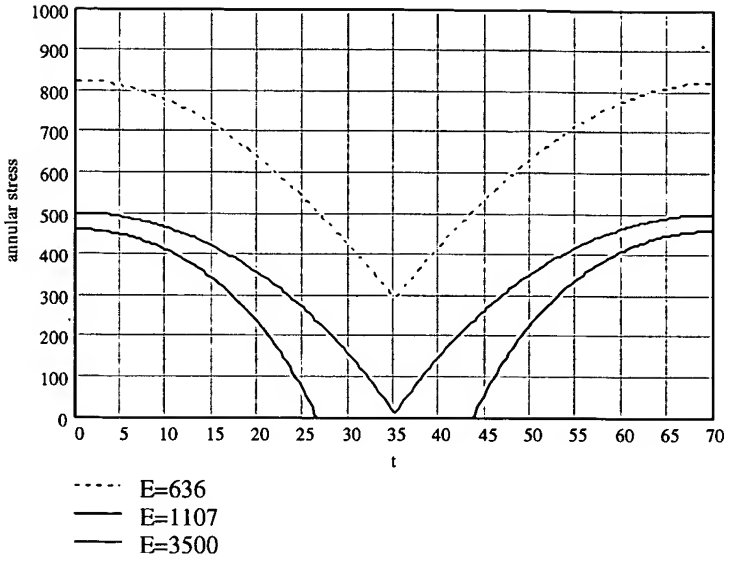

Fig. 7. Circular stresses in a pliable film. R_0=35; h=0.01; ν=0.39; p=0.2

The distribution of circular stresses is shown on Fig. 7 and Fig. 8. The circular stresses in the central areas of the shell are equal to the meridional stresses. At a distance from the central area, both circular and meridional stresses decrease. The circular stress decreases faster.

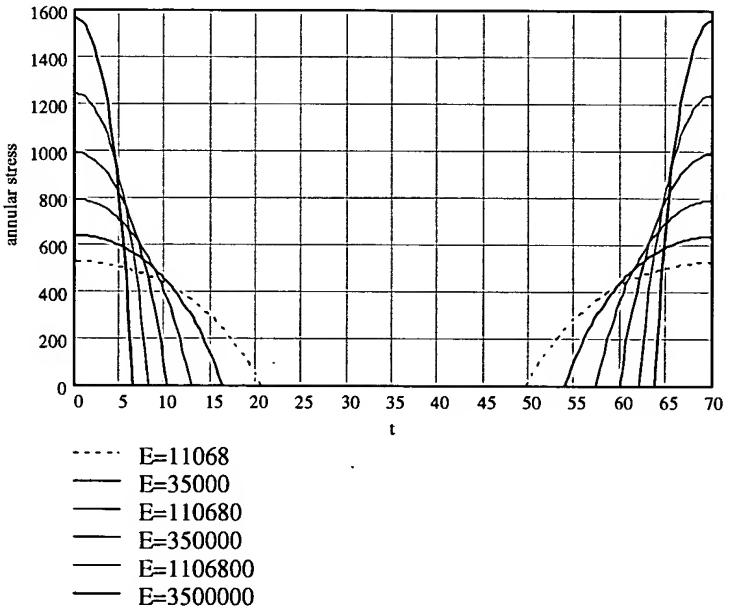

Fig. 8. Circular stresses in a rigid film. R_0=35; h=0.01; ν=0.39; p=0.2

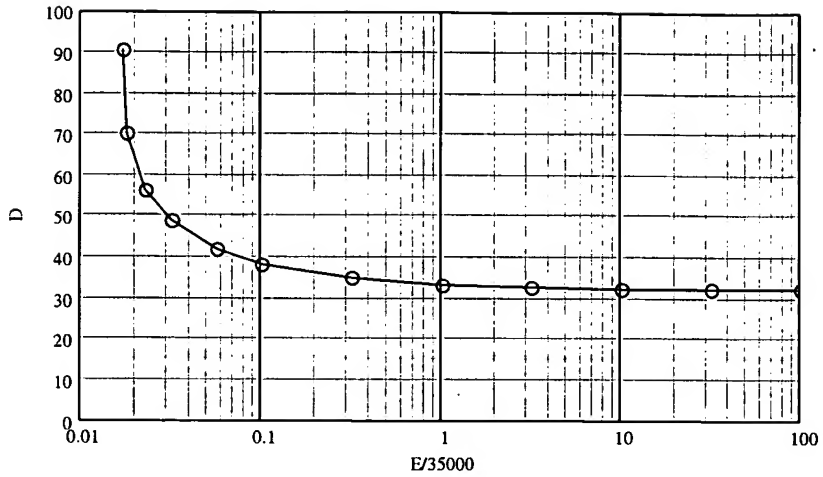

Fig. 9. Dependence of the airbag thickness D on the elasticity modulus.
R_0=35; h=0.01; ν=0.39; p=0.2

Now let's discuss the diagrams of dependence between the stress and strain parameters of the airbag and the film's tension rigidity, shown on Fig. 9 - Fig. 12. These diagrams include the relative elasticity modulus of the material along the abscissa axis. The unit of measurement is the elasticity modulus of the basic airbag design E=35000 kg-f/m^2. The logarithmic scale is used here due to a wide range of the material's rigidity variation (almost 10,000 times).

All diagrams include the critical left point that corresponds to the minimum elasticity modulus of E=593.5 kg-f/cm^2. At this point, the stable mode of equilibrium of the airbag changes to the instable mode. From the physical viewpoint, it means that the further decrease of the elasticity modulus at a specific internal pressure will result in the avalanche-like rise of deformations and the destruction of the shell.

Fig. 9 shows the diagram of the dependence of the airbag thickness D on the elasticity modulus. At large values of the elasticity modulus, the airbag thickness varies little and is about 32 to 33 cm. As the film rigidity falls down, the airbag inflates to the thickness of 90 cm, acquiring the spherical shape, and then it breaks whatever the film strength might be.

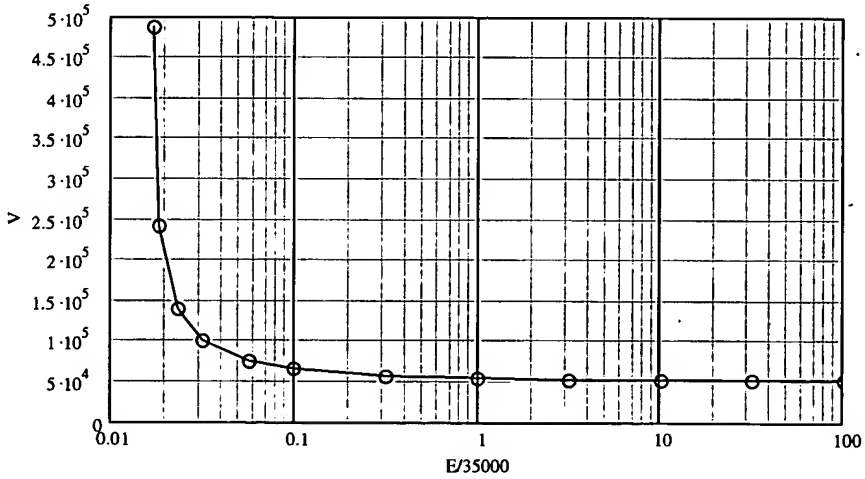

Fig. 10. Dependence between the airbag volume V and the elasticity modulus.
R_0=35; h=0.01; ν=0.39; p=0.2

The volume of the airbag that is studied (Fig. 10) made of a rigid film is 52.3 liters. The critical volume of the airbag is 488 liters.

Fold formation in the place where the round sheets are glued (Fig. 11) is intensive and absorbs about 24% of the material of the rigid film. As the rigidity goes down, folds become less clear and intensive, and they disappear at the elasticity modulus of 1150 kg-f/cm^2.

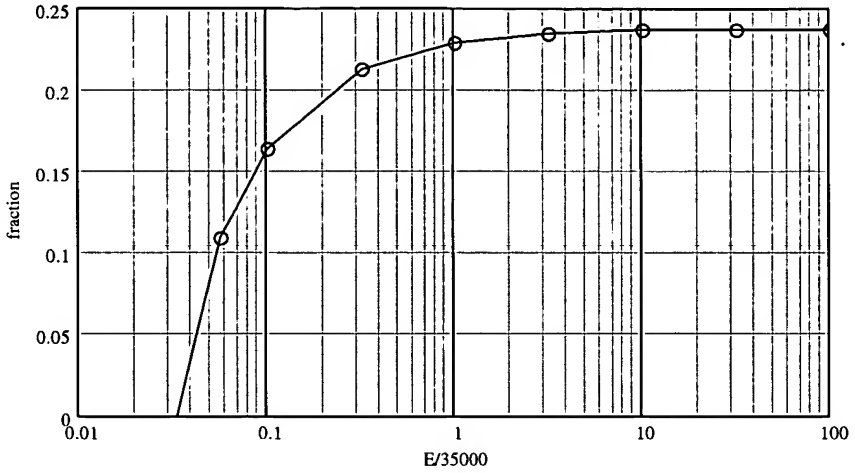

Fig. 11. Dependence of the fold formation intensity on the elasticity modulus.
R_0=35; h=0.01; ν=0.39; p=0.2

Fig. 12 shows the dependence of stresses in the bag material vs. the elasticity modulus. The solid line shows meridional and circular stresses (equal to each other) in the central area of the bag. These stresses show minimum values at the elasticity modulus of about 2000 kg-f/cm^2. The minimum value is 456 kg-f/cm^2. As the film rigidity falls, the stresses rise to the critical value of 1300 kg-f/cm^2. As the rigidity rises, these stresses also rise infinitely.

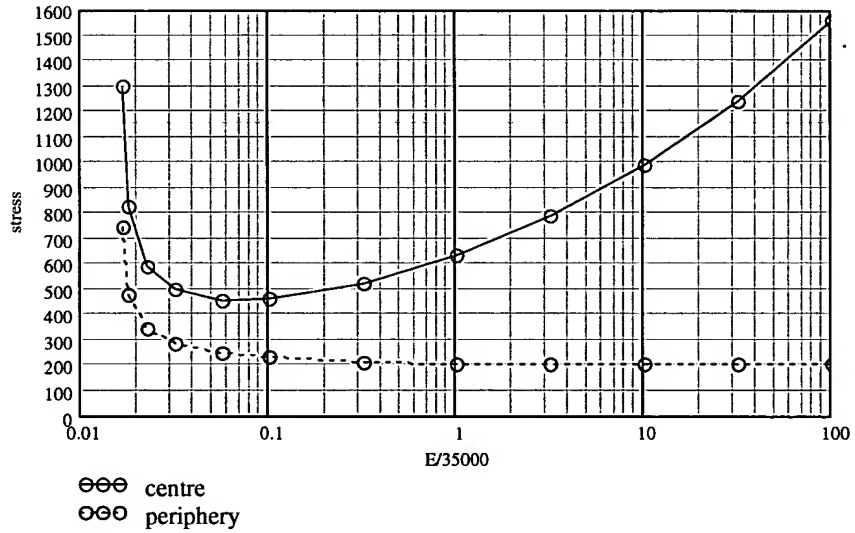

Fig. 12. Dependence of the stresses in the bag material on the elasticity modulus.
R_0=35; h=0.01; ν=0.39; p=0.2

The dotted line shows the meridional stresses in the glue seam of the film sheets. These stresses are not caused to increase by an increased film rigidity, and they tend to achieve 203 kg-f/cm^2. Their critical value is 744.5 kg-f/cm^2 at the film rigidity of 593.5 kg-f/cm^2.

3.4. Deformation of the airbag by the human body

This section studies the interaction between the airbag and the human body for the basic design of the airbag. The human body is simulated by a paraboloid of revolution (Fig. 1) with the

curvature radius in the vertex R=40 cm. Depending on the force caused by the man's pressure upon the bag, the airbag's shape, its stress and strain state, its internal volume and the depth of the man's body indentation are determined.

The shape of the airbag is shown on Fig. 13 and Fig. 14. The analysis was done with fixed values of the interaction force between the man and the airbag Q. The step of variation of this force is 50 kg-f, except for the last value of 23.5 kg-f that corresponds to a completely flat airbag.

Fold formation in all phases of flattening can be observed in the equatorial region of the airbag. At an intensive flattening, the folds appear even where the man's body touches the bag. The regions and intensities of fold formation are shown as diagrams on Fig. 15 and Fig. 16.

Just as in the case of a free airbag, the stresses show their minimum in the equatorial region, and they rise when approaching the poles. The maximum values of the stresses are found in the center of the airbag, exactly where it touches the man. The distribution of meridional stresses is shown on Fig. 17 and Fig. 18, and the distribution of circular stresses is shown on Fig. 19 and Fig. 20. Also, Fig. 21 shows diagrams of stresses in the central part of the bag vs. degree of flattening of the airbag.

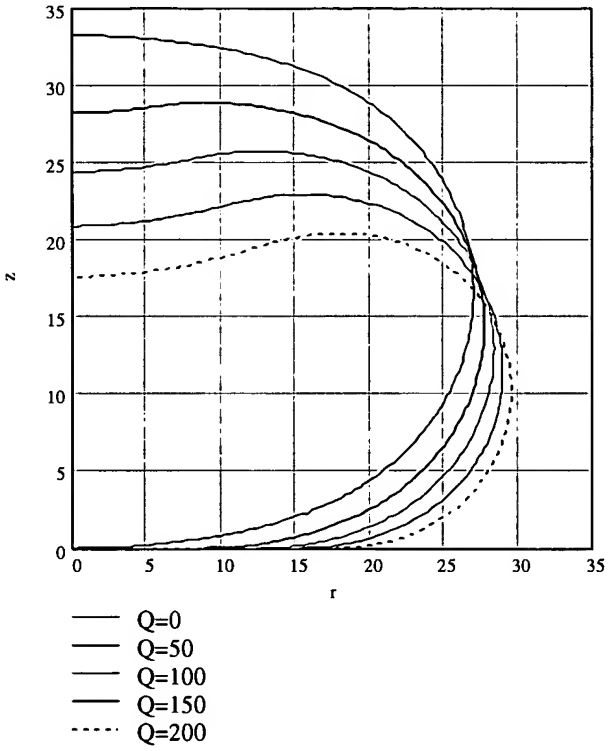

Fig. 13. Shapes of the airbag at a slight flattening
R_0=35; R=40; h=0.01; E=35000; ν=0.39; p=0.2

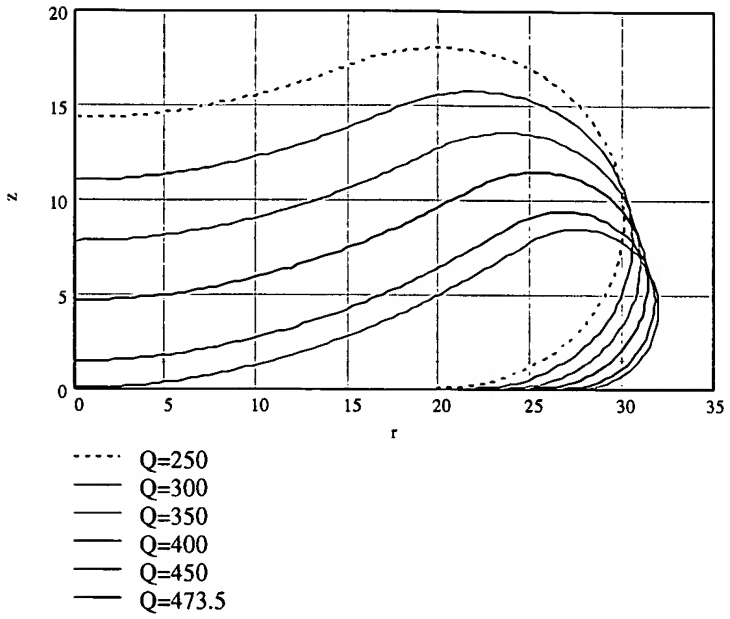

Fig. 14. Shapes of the airbag at an intensive flattening
R_0=35; R=40; h=0.01; E=35000; ν=0.39; p=0.2

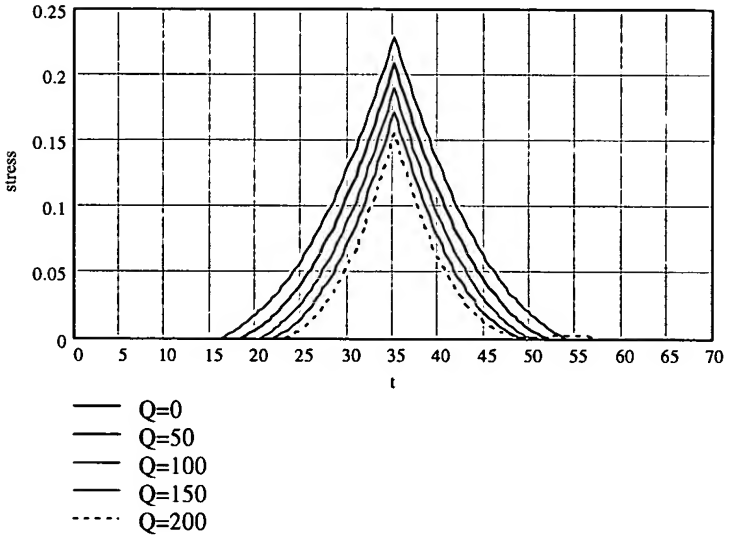

Fig. 15. Regions and intensities of fold formation at a small flattening
R_0=35; R=40; h=0.01; E=35000; ν=0.39; p=0.2

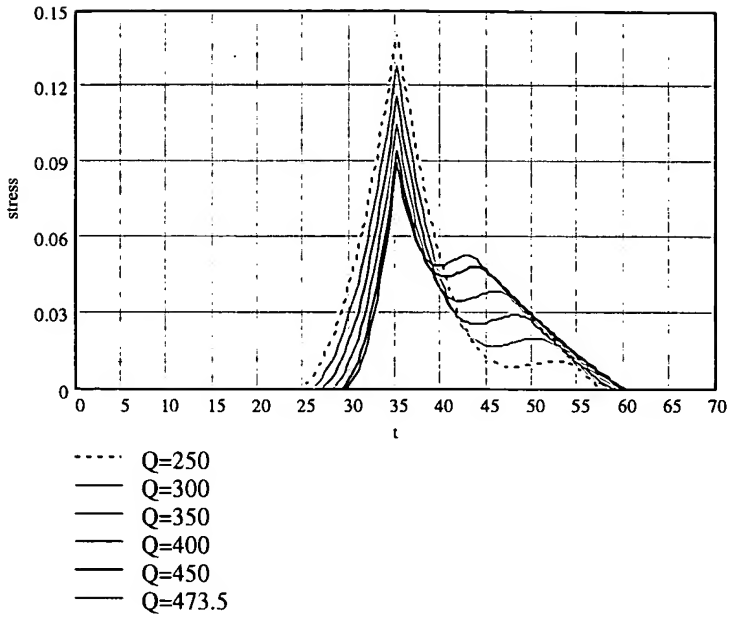

Fig. 16. Regions and intensities of fold formation at a large flattening
R_0=35; R=40; h=0.01; E=35000; ν=0.39; p=0.2

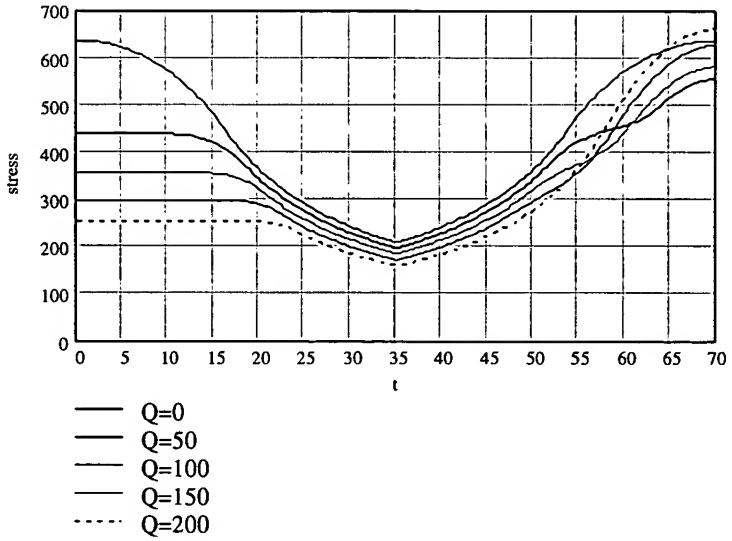

Fig. 17. Meridional stresses in the airbag at a small flattening.
R_0=35; R=40; h=0.01; E=35000; ν=0.39; p=0.2

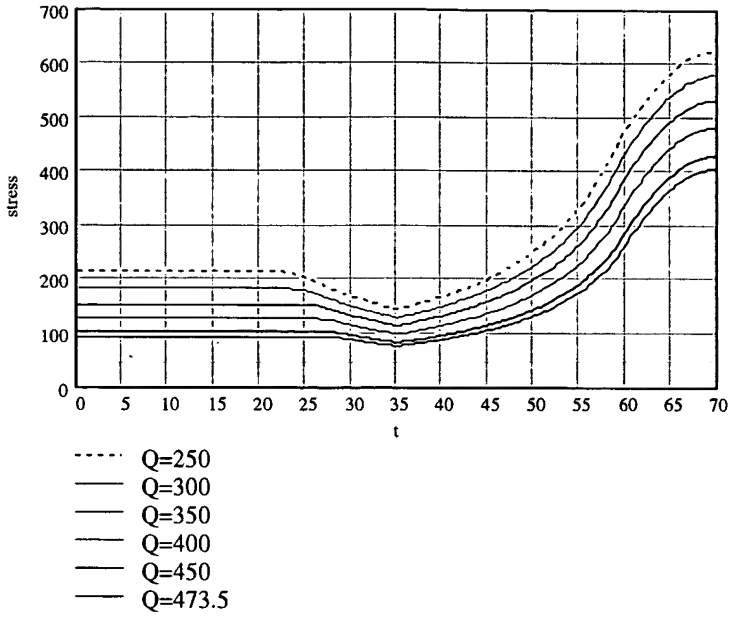

Fig. 18. Meridional stresses in the airbag at a large flattening.
R_0=35; R=40; h=0.01; E=35000; ν=0.39; p=0.2

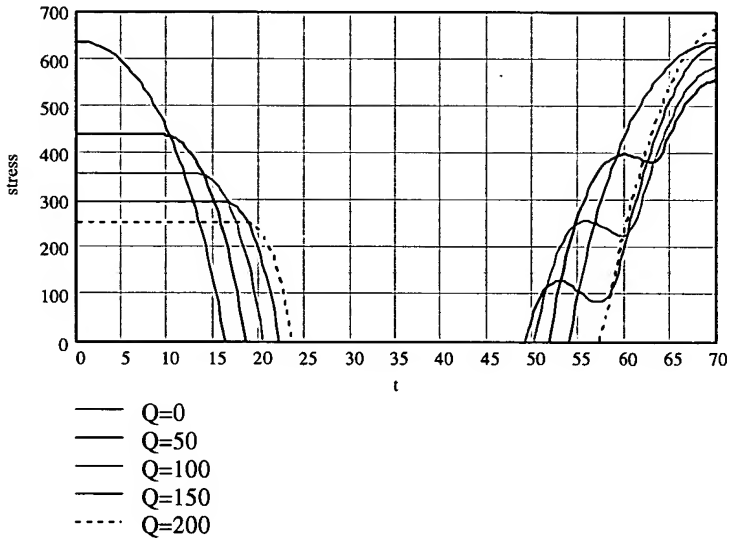

Fig. 19. Circular stresses in the airbag at a small flattening.
R_0=35; R=40; h=0.01; E=35000; ν=0.39; p=0.2

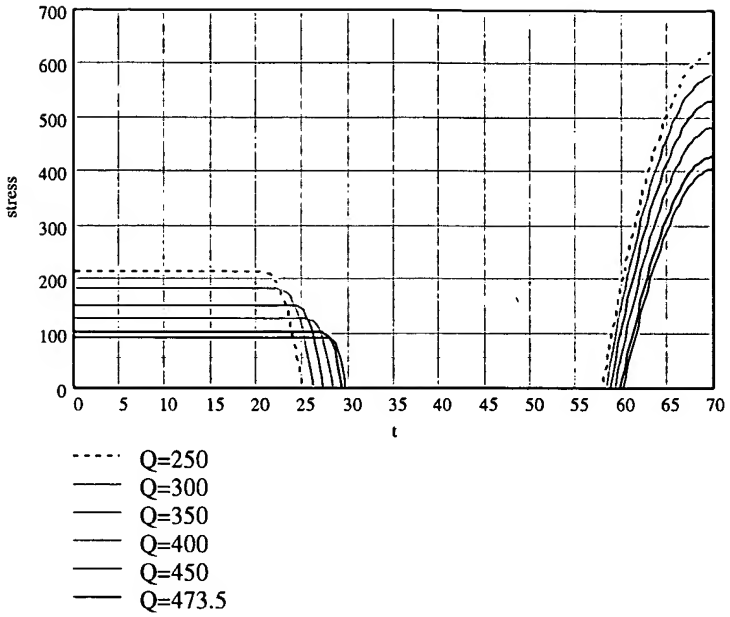

Fig. 20. Circular stresses in the airbag at a large flattening.
R_0=35; R=40; h=0.01; E=35000; ν=0.39; p=0.2

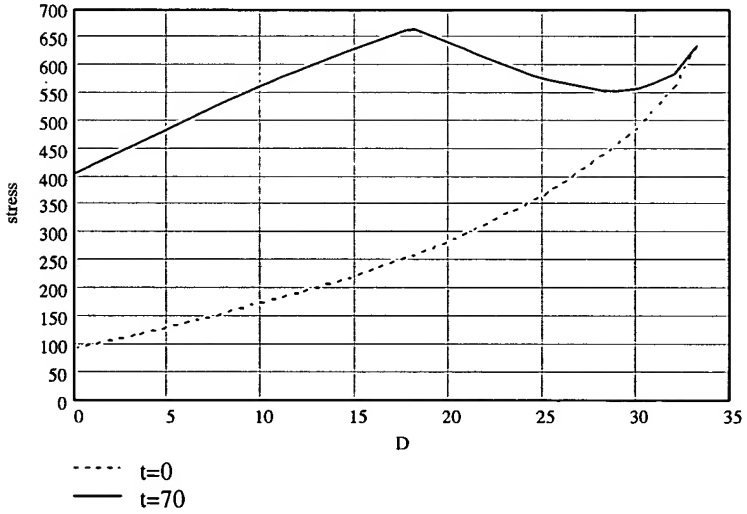

Fig. 21. Stresses in the central areas of the bag vs. the degree of the bag flattening.
R_0=35; R=40; h=0.01; E=35000; ν=0.39; p=0.2

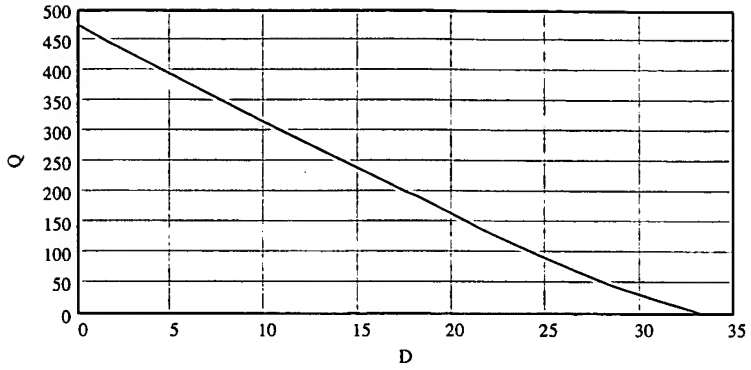

Fig. 22. The reaction force Q of the airbag vs. the degree of the bag flattening D.
R_0=35; R=40; h=0.01; E=35000; ν=0.39; p=0.2

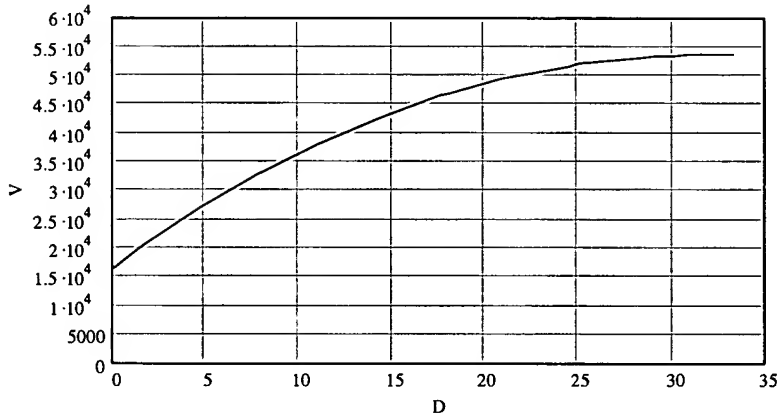

Fig. 23. The volume of the airbag V vs. the degree of the bag flattening.
R_0=35; R=40; h=0.01; E=35000; ν=0.39; p=0.2

It is much of interest to know the dependence of the airbag's volume and its reaction force on its degree of flattening. These data are necessary to solve the dynamical problem of softening the man-car impact during the car collision with a barrier. The mentioned dependences are shown on Fig. 22 and Fig. 23.

3.5. Dependence of the stress and strain state of the airbag on its internal pressure

The assumption that the strains depend little on the internal pressure while the stresses are proportional to that seems pretty reasonable. To validate this assumption, a series of problems have been solved at the following fixed initial data: R_0=35; R=40; h=0.01; E=35000; ν=0.39; D=17.5. The range of the internal pressure variation is p=0.02..2 kg-f/cm^2, that is, the topmost boundary is one hundred times the lowest pressure and the basic value is 0.2 kg-f/cm^2.

Results of this study are shown on Fig. 24 to Fig. 26. They confirm the mentioned assumption only partially.

The abscissa axes of all diagrams shows the relative variation of internal pressure within the airbag p/p_0 where p_0=0.2 kg-f/cm^2, i.e. the pressure assumed for the basic design. The ordinate axis shows values of various functions normalized for their values in the basic design.

The study shows (see Fig. 24) that, indeed, the dimensions of the airbag change little as the pressure varies. If we exclude too great a value of p=2 kg-f/cm^2 then the radial coordinate will vary within the limits of -1% .. +2%. The volume of the airbag experiences slightly larger variations, within the limits of -2% .. +5%.

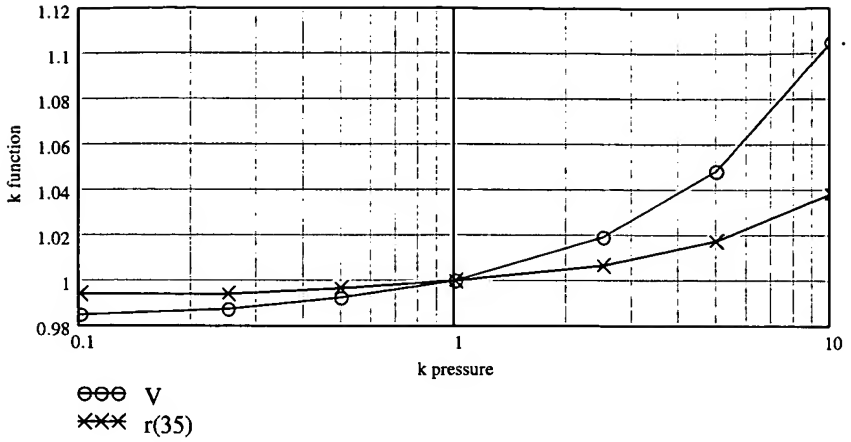

Fig. 24. Relative variation of the airbag volume V and the radial coordinate $r(35)$ at the glue seam vs. relative pressure within the airbag p

As for force/stress factors, their relative changes look like straight lines on diagrams in the logarithmic scale. It means that the dependence like that can be described by the following formula:

$$F = F_0\left(\frac{p}{p_0}\right)^a; \qquad (3.4)$$

where F is the value of the unknown function at the pressure p;

F_0 is the value of the unknown function at the pressure p_0;

a is an empirical value.

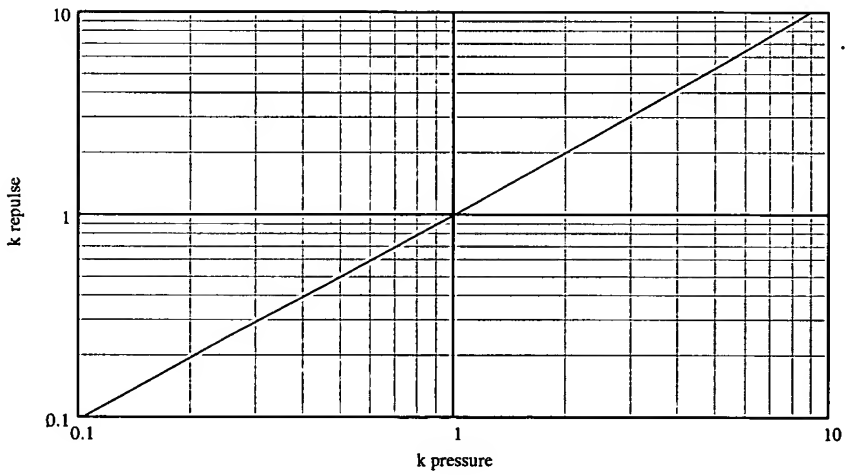

Fig. 25. Relative reaction force of the airbag Q vs. relative pressure within the airbag p

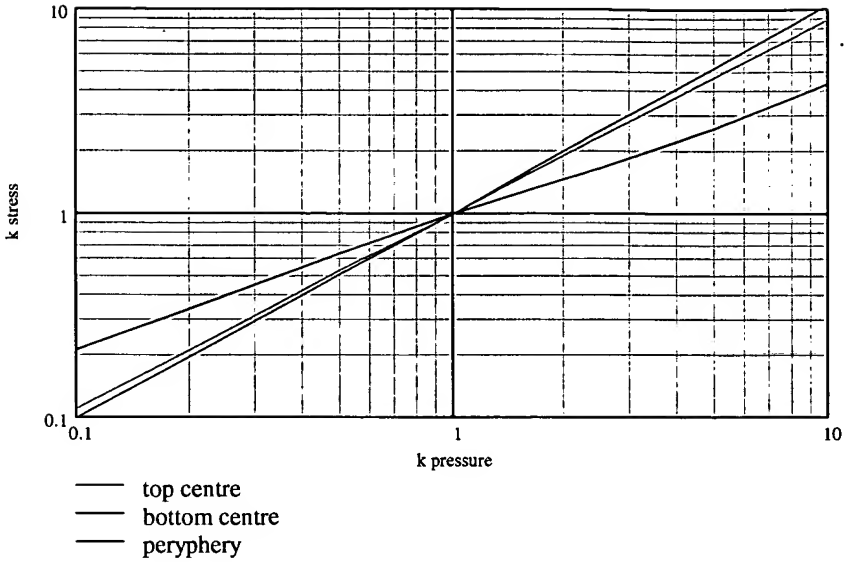

Fig. 26. Relative stresses vs. relative pressure in the airbag p

4. CONCLUSIONS

- The efficiency of the described technique for analyzing the airbag has been confirmed by a lot of practical solutions obtained.
- Results of the analysis show that the film of the thickness h=0.01 cm experiences unallowably large stresses. It is necessary to increase the thickness of the film or (and) its strength.
- Dependencies obtained in this report enable one to adjust properties of the airbag and choose a material for its fabrication.
- The dependences of the reaction force Q of the airbag and its volume on its degree of flattening D have been obtained. These dependences enable one to pose and solve a dynamical problem of interaction between a man and the airbag after the car impacts an obstacle. The solution of this dynamical problem will enable us to trace the following values in time: internal pressure within the airbag, the force of interaction between the man and the airbag, the velocity acquired by the man when pushed off by the airbag, and other physical parameters.

5. REFERENCES

[1]. Sanders. Analysis of Film Airbag. Sanders.doc. 2000.

[2]. S.A.Alexeyev. A basic theory of soft axisymmetric shells. In book: Analysis of spatial structures, vol.10, Moscow: *Stroyizdat*, 1965. (*In Russian*)

[3]. Kyuichiro Washizu. Variational Methods in Elasticity and Plasticity. Third edition. Pergamon Press. Oxford, New York, Toronto, Sydney, Paris, Frankfurt, 1982.

[4]. L.S. Pontryagin, V.G. Boltyanski, R.V. Gamkrelidze, E.F. Mischenko. Mathematical theory of optimum processes. Moscow, "Nauka", 1969. (*In Russian*)

[5]. G.A.Korn, T.M.Korn. Mathematical Handbook for Scientists and Engineers. Second, enlarged and revised edition. McGraw-Hill Book Company. New York, San Francisco, Toronto, London, Sydney, 1968.

[6]. I.N. Bronstein, K.A. Semendiayev. Mathematical handbook for engineers and students of engineering. 13th edition, revised. Moscow, "Nauka", 1986. (*In Russian*)

[7]. V. Diakonov. Special reference guide. Mathcad 8/2000. "Piter" Publishers. St.-Petersburg, Moscow, Kharkiv, Minsk, 2000. (*In Russian*).